Critical-state flux penetration and linear microwave vortex response in $YBa_2Cu_3O_{7-\delta}$ films

Balam A. Willemsen*
Physics Department, Northeastern University, Boston, Massachusetts 02115
and Rome Laboratory, Hanscom AFB, Bedford, Massachusetts 01731

J. S. Derov
Rome Laboratory, Hanscom AFB, Bedford, Massachusetts 01731

S. Sridhar
Physics Department, Northeastern University, Boston, Massachusetts 02115
(Received 22 May 1997)

The vortex contribution to the dc magnetic field (H) dependence of the microwave surface impedance $\tilde{Z}_s(H)=R_s(H)+iX_s(H)$ of $YBa_2Cu_3O_{7-\delta}$ thin films was measured using suspended patterned resonators. $\tilde{Z}_s(H)$ is shown to be a direct measure of the flux density $B(H)$ enabling a very precise test of models of flux penetration. Three regimes of field-dependent behavior were observed: (1) Initial flux penetration occurs on very low-field scales $H_i(4.2\ \mathrm{K})\sim 10$ mT, (2) at moderate fields the flux penetration into the virgin state is in excellent agreement with calculations based upon the *field-induced* Bean critical state for thin-film geometry, parametrized by a field scale $H_s(4.2\ \mathrm{K})\sim J_c d\sim 0.5$ T, and (3) for very high fields $H\gg H_s$, the flux density is uniform and the measurements enable direct determination of vortex parameters such as pinning force constants α_p and vortex viscosity η. However, hysteresis loops are in disagreement with the thin-film Bean model, and instead are governed by the low-field scale H_i, rather than by H_s. Geometric barriers are insufficient to account for the hysteresis loops. [S0163-1829(97)08641-4]

I. INTRODUCTION

The dynamics of vortices is important over a wide spectrum of time scales (or frequencies). On very long time scales the problem is relevant to dissipation at or near the critical current. On the other end of the spectrum, at short time scales or high frequencies, an understanding of vortex dynamics is important both for fundamental understanding and for practical applications of microwave devices.

Yet another need is to understand flux profiles and field penetration into thin films. Recently there have been several calculations based upon critical-state models which have yielded field and current distributions in thin films for magnetic fields applied perpendicular to the films, and have shown that there are qualitative differences from bulk geometries. While some of these results have been tested in actual experiments,[1] not all aspects of these models are fully understood. Most experimental studies of flux penetration and the critical state have involved measurements of magnetic properties such as the dc magnetization, and there are few investigations of the dynamic properties.

This paper reports on a different approach, utilizing microwave surface impedance measurements in patterned microstrip resonators, to understanding vortex dynamics and flux penetration. Specially designed microstrip resonators patterned from thin films are used as high Q structures to probe vortex response at microwave frequencies in the presence of dc magnetic fields. The high sensitivity of these structures enables measurement of the vortex response in fields from <0.1 mT to several T. The complex microwave surface impedance $\tilde{Z}_s=R_s+iX_s$ was measured as functions of magnetic field H, temperature T, and frequency ω (in the range 1 to 20 GHz). $\tilde{Z}_s$ is a measure of the total flux in the sample, and hence can lead to precise tests of flux penetration in thin films. In addition the results also yield information on vortex parameters such as pinning force constants and viscosity.

In this paper we focus on results for the changes in surface impedance induced in $YBa_2Cu_3O_{7-\delta}$ (YBCO) thin films as the externally applied magnetic field is slowly increased from zero, as well as the hysteresis loops which ensue when the field is subsequently reduced. The response clearly shows evidence of two relevant field scales. As the field is increased an initial linear rise gives way to a superlinear behavior at H_i followed by a linear rise above H_s which persists to the highest fields available. While virgin response for $H>H_i$ and the magnitude of H_s appear to be consistent with recent analytical expressions for thin strips in perpendicular fields, the hysteretic response is not so easily understood. The critical state model predicts a counterclockwise hysteresis loop governed by a field scale of order H_s, while the experiments observe a clockwise hysteresis loop governed by the much smaller field scale H_i. Geometrical barriers are insufficient to explain the observed hysteresis loops. The results suggest that pinning at the film edges may be weaker than in the bulk.

II. EXPERIMENTAL DETAILS

The experiments were designed specifically to enable high sensitivity measurements in dc magnetic fields from <0.1 mT to several T. The essential element is the suspended line resonator, fabricated using YBCO films deposited using pulsed laser deposition techniques onto $LaAlO_3$

substrates, and housed in a Cu package. Microwaves are coupled in inductively, by means of loops at the ends of coaxial lines. Similar resonators were used in studies of high field[2] and nonlinear[3] response, which have already been published. We note several key features of the experiment.

The absence of superconducting ground planes (such as would be present in a traditional stripline or microstrip resonator) allows us to observe effects even at very low applied magnetic fields since there is no magnetic shielding associated with the ground planes.

The presence of several modes enables measurements at several frequencies in the 1–20 GHz range.

The ability to carry out both linear and nonlinear response experiments independently, and also combined rf+dc field experiments where the rf and dc field scales are comparable.

Variable coupling at all temperatures enabling weak coupling over a broad range of resonator Q's.

Experiments were initially carried out in fields of $1\,\mathrm{mT} < \mu_0 H < 4\,\mathrm{T}$ in a Janis SuperVaritemp Helium flow cryostat. The magnetic fields were generated using a NbTi coil (capable of fields up to 6 T) which is permanently mounted in the cryostat. Current was supplied to the solenoid by a Cryomagnetics IPS-50 Magnet Power Supply, under computer control via RS-232 using a Cryomagnetics CIM-16. Magnet calibration runs using a LakeShore 450 Gaussmeter and a 5 ft cryogenic axial Hall probe showed that residual fields of the order of 1–10 mT may be present at the center of the superconducting NbTi magnet once it had been energized. For experiments at true zero applied static field, and for greater sensitivity at low fields the probe was adapted to fit in a similar flow cryostat built by Cryo Industries of America. In this series of low-field experiments, the magnetic fields were supplied by a liquid N_2 cooled Cu solenoid capable of fields up to 40 mT when supplied using an HP 6024A power supply. The CIM-16 interface module was also used here to control the supply current remotely via RS-232. Current (and hence field) reversal was accomplished by manually interchanging the magnet leads at zero current. The field-to-current ratio was determined using a LakeShore 450 Gaussmeter and an axial probe to be 10.6 ± 0.1 mT/A.

A number of additional features were incorporated into the probe in order to increase the system's sensitivity at low magnetic fields. A Minco thin-film heater with a nominal resistance of 50Ω was attached to the bottom of the package with GE 7031 varnish in order to improve the temperature control, and hence long term stability required for this work. The temperature of the vaporizer was controlled with a LakeShore DR-91C Temperature Controller and a calibrated CGR-1-2000 carbon-glass sensor, while the sample temperature was controlled with a LakeShore DR-93C Temperature Controller and a calibrated CGR-1-2000 carbon glass sensor. In order to achieve long term temperature stability, the heater on the vaporizer was set to attain temperature slightly below the desired measurement point; the heater on the package was used to fine-tune and stabilize the temperature. Thus, temperature stability of ~ 1 mK could be obtained and held for hours, enabling extremely detailed study of $\tilde{Z}_s(H)|_{\omega,T}$.

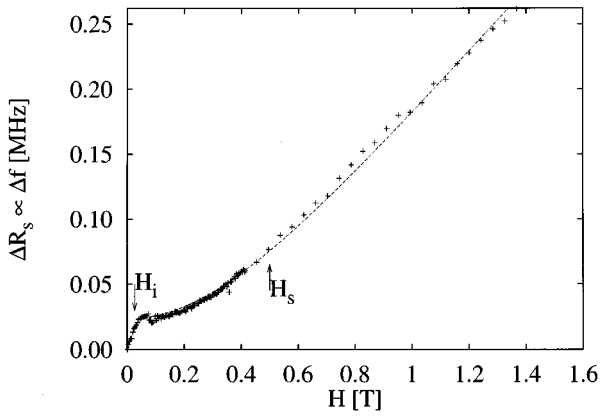

FIG. 1. Typical virgin state response: Raw Δf data for increasing applied field for a sample initially in the virgin state for resonator N3 at 3.7 GHz and 5 K. The dashed line is the expression of Eq. (10). The arrows indicate the two field scales, H_i and H_s.

The microwave transmission amplitude S_{21} of the fully assembled system was measured using an HP 8510C Automatic Network Analyzer (ANA). All data acquisition and computer control was carried out on an HP 745i workstation running HP VEE.

In order to obtain data at these low-field scales it becomes essential to go beyond simply characterizing the resonance by measuring the resonance frequency f_0 and the 3 dB bandwidth $\Delta f_{3\ \mathrm{dB}}$ and hence the quality factor $Q = f_0/\Delta f_{3\ \mathrm{dB}}$. Thus we developed a least squares analysis to fit our resonances to a Lorentzian form. The results of these fits were found to agree very well with the values obtained from the standard 3 dB method, but provided significantly enhanced sensitivity to small changes.

The changes in surface impedance associated with the application of magnetic field are extracted from the measured quantities as follows:

$$\Delta\tilde{Z}_s(H,T) = \tilde{Z}_s(H,T) - \tilde{Z}_s(H=0,T) = \Gamma[\Delta f_{3\ \mathrm{dB}}(H,T) - \Delta f_{3\ \mathrm{dB}}(H=0,T) + i2(f_0(0,T) - f_0(H,T))], \tag{1}$$

where Γ is a geometric factor determined from the sample dimensions. (See Table I.) Figure 1 shows typical data for Δf, which is proportional to R_s, as the applied dc field is varied starting from zero field for the sample in a zero-field cooled virgin state.

TABLE I. The two resonators used for this work.

Resonator	Geometry	Linewidth	Resonator length	Film thickness	Substrate thickness
N4	Straight	100 μm	1.32 cm	0.38 μm	250 μm
N3	Ring	100 μm	2.00 cm	0.375 μm	500 μm

III. THEORY

A. Microwave vortex dynamics

Viscoelastic models of microwave vortex dynamics, such as those developed early on by Gittleman and Rosenblum[4] and later by Coffey and Clem[5] consider the effects of the Lorentz force which is exerted on the vortices by the microwave currents as the main source of an increase in surface impedance in the presence of magnetic fields. The applicability of these models has been validated in earlier experiments on a variety of crystals and films.[6–9]

We have shown in Ref. 2 that the field induced changes in surface impedance of a superconducting thin film can be well described using a simple model of vortex dynamics and parameters which are consistent with measurements on YBCO single crystals,[7] with

$$\Delta\tilde{Z}_s(H,T)=\frac{i2\omega\phi_0}{\mu_0 d[\kappa_s(T)+i\omega\eta(T)]}B(H), \qquad (2)$$

where d is the film thickness, κ_s is the pinning force constant, and η is the flux viscosity. At high fields $B(H)\rightarrow\mu_0 H$, but this is clearly not the case at low fields or in the presence of bulk pinning where the field profile in the sample can be nonuniform. It should also be noted that the increases in surface impedance due to penetrated flux must be insensitive to the sign of that flux. Thus, it is insufficient to simply replace $B(H)$ with an average flux density $\overline{B(H)}\equiv\Phi/S\equiv(1/S)\int_S B(H)dS$, where S is the surface of the sample perpendicular to the applied field. The desired quantity is the average *absolute* flux density, $\overline{|B(H)|}\equiv(1/S)\int_S|B(H)|dS$. Thus, $\Delta\tilde{Z}_s(H,T)$ can be thought of as counting the absolute number of vortices in the sample since it is directly proportional to $\overline{|B(H)|}$. Hence for nonuniform flux profiles, the above equation is modified to

$$\Delta\tilde{Z}_s(H,T)=\frac{i2\omega\phi_0}{\mu_0 d[\kappa_s(T)+i\omega\eta(T)]}\overline{|B(H)|}, \qquad (3)$$

B. Critical-state flux penetration models

The penetration of magnetic flux into a superconductor depends crucially on two elements, geometry and pinning. These are both incorporated in what is usually called the critical-state model, originally due to Bean.[10] Bulk pinning is described in terms of the critical current J_c, while the field profiles depend heavily on the sample geometry. We will compare the results for the more traditional slab geometry in a longitudinal field to those for a thin strip in a perpendicular field.

In the following we assume that H_{c1} is negligible (i.e., that flux penetrates for all fields), and that $J_c(B)=J_c(0)$ (sometimes referred to as the Bean-London model). Although hysteresis loops are usually described in terms of the magnetization $M(H)$, the average absolute induced flux density $\overline{|B(H)|}$ is the relevant parameter to use in our case, as described above.

1. Bulk geometries (slab)

For a slab of infinite extent of width W, the flux profiles can easily be written down,[11] and one can immediately compute $\overline{|B(H)|}=(1/W)\int_{-W/2}^{W/2}|B(x)|dx$. When all vortices point in the same direction, $\overline{|B(H)|}=\Phi/W\equiv(1/W)\int_{-W/2}^{W/2}B(x)dx$, where Φ is the induced flux per unit length in the sample. As the applied field is increased flux penetrates gradually from the edges of the slab, until a characteristic field $H_{s,\mathrm{bulk}}=J_c W/2$ is reached and the two flux fronts meet at the center of the slab. For increasing field applied to a slab initially in the virgin state

$$\overline{|B(H)|}=\begin{cases}\dfrac{1}{2}\dfrac{H^2}{H_{s,\mathrm{bulk}}}, & \text{for } H<H_{s,\mathrm{bulk}}\\[2ex] H-\dfrac{1}{2}H_{s,\mathrm{bulk}}, & \text{for } H>H_{s,\mathrm{bulk}}.\end{cases} \qquad (4)$$

When the field is reduced after reaching a maximum field $H_{\max}>H_{s,\mathrm{bulk}}$, the field and current profiles can be constructed using a simple construction.

$$f_{\downarrow}(x,H,H_{s,\mathrm{bulk}},H_{\max})=f(x,H_{\max},H_{s,\mathrm{bulk}})-f(x,H_{\max}-H,2H_{s,\mathrm{bulk}}), \qquad (5)$$

where f can be any of the following quantities J, B, or M. $f_{\downarrow}$ is that same quantity as the field is reduced from $H_{\max}$. Thus, as the applied field is reduced, the flux density at the edges is gradually reduced. At $H=0$ the standard sandpile flux profile can be found at the center of the sample. As the field is now increased in the other direction, negative vortices enter at the edges but the positive vortices at the center remain until $|H|>H_{s,\mathrm{bulk}}$. The curvature in the response arises from the insensitivity to direction of flux, and would not be observed in quantities such as $M(H)$ or $\Phi(H)$. The calculated hysteresis in $\overline{|B(H)|}$ for a slab is shown in Fig. 2.

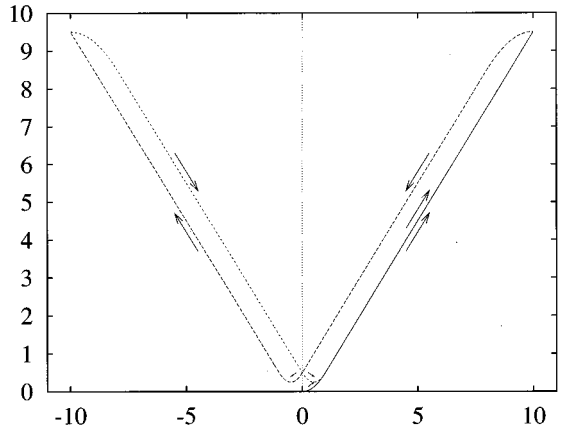

FIG. 2. The calculated hysteresis in $\overline{|B(H)|}$ for a thick slab in a field applied parallel to its surface. Both axes are in units of $H_{s,\mathrm{bulk}}$, with $H_{\max}=10H_{s,\mathrm{bulk}}$.

2. Thin film in a perpendicular magnetic field

A number of theorists[12–15] have recently studied the problem of thin strips or disks in a perpendicular magnetic field, using conformal mapping techniques introduced early on by Norris.[16] Analytic solutions for the current and flux density distributions in the strip are thus now becoming available for this problem, which could heretofore only be considered numerically.

In what follows we will briefly summarize the central results of Ref. 12 recast in a form which better suits our purposes. Again, as in the case of the traditional Bean model for bulk geometries we ignore H_{c1} and assume that $J_c(B)=J_c(0)$.

The geometry is that of an infinitely long strip of thickness d and width $2a$ aligned such that the sample lies in the xy plane with its width along the $\hat{y}$ axis. In the Meissner state the current distribution must be such that $B_z(y)=0$ for $|y|<a$.

If flux can now penetrate to a distance $b<a$, the current distribution must change. b can be determined by imposing the condition that $J(b)$ is finite, as well as the boundary condition on B [$B(x)=\mu_0 H$ far away from the sample]. This leads to $b=a/\cosh(H/H_{s,\mathrm{strip}})$, where $H_{s,\mathrm{strip}}$ is now a characteristic field related to the critical current and the geometry, $H_{s,\mathrm{strip}}=J_c d/\pi$. It should be noted that unlike at $H_{s,\mathrm{slab}}$ in the case of a slab, the two flux fronts do not meet at $H=H_{s,\mathrm{strip}}$. In fact, b is always nonzero for finite fields, although at some point b will be smaller than the effective size of a single vortex λ and the validity of these expressions must be questioned. The resulting sheet current distribution can then be written as

$$K_x(y)\equiv\int_{-d/2}^{d/2}J_x(z,y)\,dx = \begin{cases} \dfrac{2J_c d}{\pi}\tan^{-1}\dfrac{y\sqrt{a^2-b^2}}{a\sqrt{b^2-y^2}}, & \text{for } |y|<b \\ J_c d\,\dfrac{y}{|y|}, & \text{for } b<|y|<a. \end{cases} \tag{6}$$

$$B_z(y)=\begin{cases} 0, & \text{for } |y|<b \\ \mu_0 H_c\tanh^{-1}\dfrac{a\sqrt{y^2-b^2}}{|y|\sqrt{a^2-b^2}}, & \text{for } b<|y|<a \\ \mu_0 H_c\tanh^{-1}\dfrac{|y|\sqrt{a^2-b^2}}{a\sqrt{y^2-b^2}}, & \text{for } a<|y|. \end{cases} \tag{7}$$

It should be noted that $B_z(y)$ has a logarithmic singularity at the edges in this expression.

Thus, we can use Eq. (7) to evaluate

$$\overline{|B(H)|}=(1/2a)\int_{-a}^{a}B(y)\,dy=\mu_0 H_{s,\mathrm{strip}}\ln\cosh\frac{H}{H_{s,\mathrm{strip}}}. \tag{8}$$

Note that this has some striking similarities with the results for the slab geometry: (i) a characteristic field scale ($H_{s,\mathrm{bulk}}$ or $H_{s,\mathrm{strip}}$) related to the critical current density, (ii) $\overline{|B(H)|}\propto H^2$ at low fields $H\ll H_s$, and (iii) $\overline{|B(H)|}\propto H$ at high fields $H\gg H_s$.

Assuming that Eq. (5) applies just as for the slab, the hysteretic response can be constructed with $H_{s,\mathrm{strip}}$ taking the place of $H_{s,\mathrm{bulk}}$, and is presented in Fig. 3.

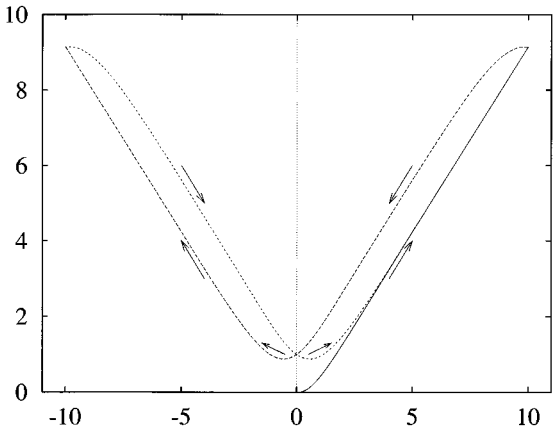

FIG. 3. Hysteretic response in $\overline{|B(H)|}$ for a thin strip in a perpendicular field calculated numerically from the field profiles discussed in the text. Both axes are in units of $H_{s,\mathrm{strip}}$, and $H_{\max}=10H_{s,\mathrm{strip}}$.

IV. $\widetilde{Z}_S(H)$: EXPERIMENTAL RESULTS

All of the results presented here were obtained with the sample at fixed temperature, and initially in the virgin state. This allows us to separate out the initial penetration of flux from the overall response and hysteresis which is observed at higher fields. The sample was warmed up well above T_c and cooled down in zero field between runs in order to ensure that the sample was really in the virgin state.

The data for the virgin state flux penetration from $<100\mu$ T to 6 T fall naturally into three field regimes.

(1) Changes occur initially on very small field scales which we call $\mu_0 H_i(4.2\text{ K})\sim 10$ mT.

(2)This is followed by the majority of the flux penetration at field scales of around $\mu_0 H_s(4.2\text{ K})\sim 500$ mT characterized by a superlinear dependence of the impedance on H, and indicating an inhomogeneous flux distribution.

(3) At very high fields $H\gg H_s$ the dependence of $\widetilde{Z}_s(H)$ becomes linear in H indicating uniform flux penetration.

A. Initial penetration of flux

The detailed behavior up to 40 mT at 4.2 K is presented in Fig. 4, where it can clearly be seen to be characterized by a field scale $\mu_0 H_i(4.2\text{ K})\sim 10$ mT, and that above and below H_i the impedance appears to be approximately linear. The actual dependence is well described by the functional form:

$$\overline{|B(H)|}=C_i\tanh(H/H_i)+C_l H \tag{9}$$

and is shown in the figure as a solid line. This functional form is obtained empirically and is not described at present by any microscopic model. The value of H_i used in the fit is indicated by an arrow.

It is easy to extract H_i from the data by a linear extrapolation of the behavior above and below the bend, and its temperature dependence is presented in Fig. 5. H_i is chosen to be the intersection point of these two lines. This is nearly equivalent to the field scale H_i that enters in Eq. (9), but does not presuppose any specific functional dependence of $\widetilde{Z}_s(H)$ at low fields.

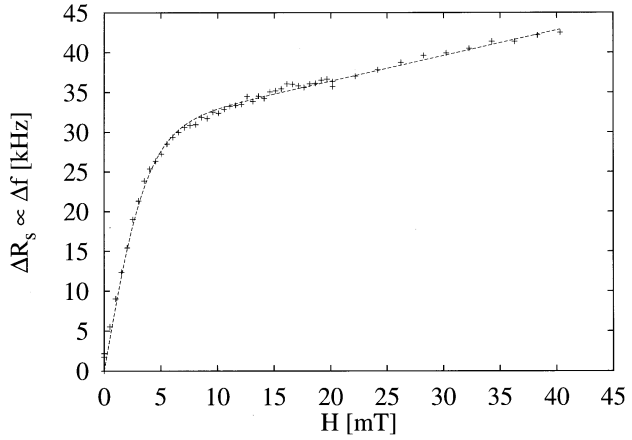

FIG. 4. Typical virgin state response: Raw Δf data for increasing applied field for a sample initially in the virgin state for resonator N4 at 3.7 GHz and 5 K. The dashed line is the expression of Eq. (9). The arrow indicates the field scale described in the text.

Is this low-field scale simply a manifestation of H_{c1}? H_{c1} is typically observed as a sharp break from practically zero in microwave measurements, due to the logarithmic singularity in $B(H)$ near H_{c1}. This is not what is seen in Fig. 4. However, the magnetic field $H_{c1,\mathrm{strip}}$ at which flux initially penetrates into a thin strip in a perpendicular magnetic field will in general be lower than the bulk H_{c1} of the material, due to demagnetization effects. Using standard ellipsoidal approximations to a thin strip yields an estimate of $H_{c1,\mathrm{strip}}=H_{c1}(d/2a)$. Recent analytical calculations[14,17] find that the effect is actually smaller than that predicted by the ellipsoidal approximation by a factor of $\sqrt{d/2a}$, so that $H_{c1,\mathrm{strip}}=H_{c1}\sqrt{d/2a}$. For a 0.5 μm$\times$100 μm strip, typical of those used for these experiments, one finds that $H_{c1,\mathrm{strip}}\sim H_{c1}/10$.

Bulk H_{c1} for single crystalline YBCO was measured by Wu *et al.*[7] where they found that $\mu_0 H_{c1,\|}(0)=85\pm4$ mT, leaving us with an upper bound on the penetration field $\mu_0 H_{c1,\mathrm{strip}}\sim 8.5\pm0.4$ mT for our samples. This magnitude is comparable to the observed low-temperature magnitude of H_i.

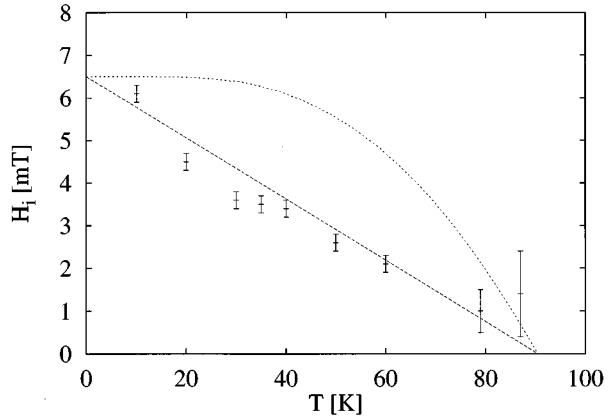

FIG. 5. Temperature dependence of the initial penetration field scale for resonator N4. The straight dashed line is a least squares fit to the data. The dotted line presents a BCS temperature dependence for H_{c1}.

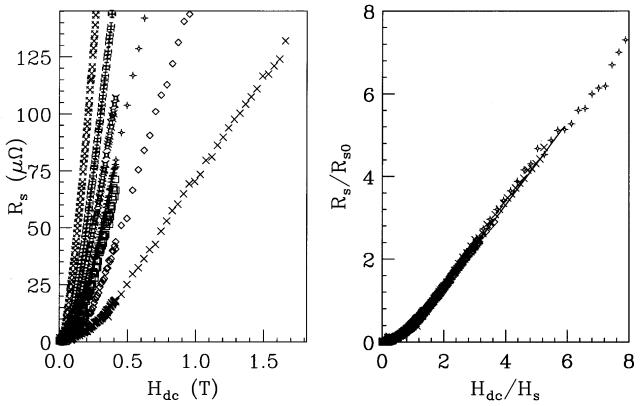

FIG. 6. Raw (left) and scaled (right) plot of the field induced changes in surface resistance $R_s(H)$. Data presented is for resonator N3 at 3.7 GHz and T=(5.0, 15.0, 20.0, 25.0, 31.0, 40.0, and 50.0 K). The slope increases with increasing T temperatures. The solid line represents the expected behavior for a strip (eq. of text). A dashed line representing the expected behavior for a disk is also presented, but is indistinguishable from the solid line.

If H_i is simply a manifestation of H_{c1}, the linear field dependence below H_i is somewhat unconventional. For a conventional GL superconductor, the effects of pair breaking are expected to have a quadratic field dependence below H_{c1}.[18,19] This quadratic dependence has also been observed experimentally in radio frequency penetration depth measurements on polycrystalline samples[20] and single crystals of YBCO (Ref. 7) for fields applied parallel to the ab plane. It should also be mentioned that Yip and Sauls[21] have shown that for a d-wave superconductor, the penetration depth (and hence also the surface resistance) should rise linearly in the Meissner state. Other measurements of H_{c1} on single cystals of YBCO have been reported[22] which are consistent with these theoretical predictions, and thus the thin film measurements presented here.

1. H_{c1} and weak links

A quadratic field dependence is also expected from the weakly coupled-grain model,[23,24] which has been used to explain the functional dependence of $\tilde{Z}_s$ on low microwave fields. Certain theories for granular superconductors do predict an initial linear field dependence[25,26] by considering a Bean-like model applied to the intergranular weak links. Weak links are proposed as an explanation for a similar initial linear rise followed by a saturation reported in the literature.[27] We looked for, but did not find any direct correlation between film granularity and the magnitude of H_i. Films of very different granularity (as evidenced by the rate at which the films etched) had remarkably similar magnitudes of H_i. Thus, the linear dependence on field cannot conclusively be attributed to the presence of weak links in the samples.

B. Scaling of the data for moderate fields

The field induced change in surface impedance, $\Delta\tilde{Z}_s(H,T,\omega)=\tilde{Z}_s(H,T,\omega)-\tilde{Z}_s(H\rightarrow0,T,\omega)$ at moderate fields ($\mu_0 H_i<\mu_0 H<4T$) can be scaled, as shown in Fig. 6,

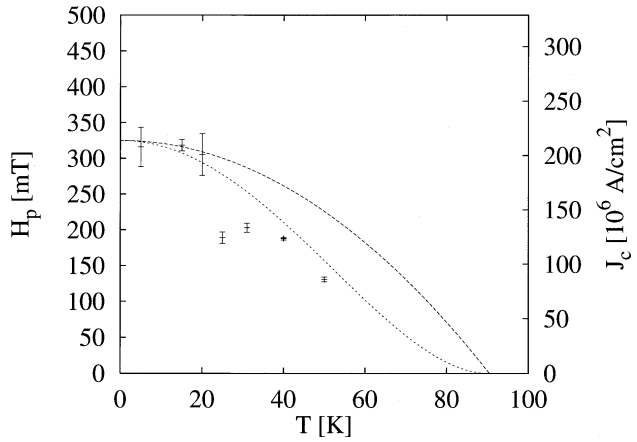

FIG. 7. Field scale H_s for the ring resonator N3 at 3.7 GHz. The dashed and dotted lines are $(1-t^2)$ and $(1-t^2)^2$ dependences, respectively. The equivalent scale for the corresponding critical current density $J_c(T)=H_s\pi d$ is also shown on the right axis.

giving a field scale H_s and an impedance scale which can be determined from the slope at high fields.

The scaled data over this broad field range are well described by the following expression:

$$\overline{|B(H)|}=C_s \ln\cosh(H/H_s), \tag{10}$$

where H_s is the field scale well above which the flux has largely penetrated throughout the sample and $B(H)\approx\mu_0 H$ (solid line in right panel of Fig. 6).

The scaling function used above is exactly that obtained from the critical-state model of rectangular strips presented in Sec. III B 2. This would imply that J_c must depend only weakly on H, and only one field scale [related to $J_c(T)$] determines the response. Thus, we should now be able to estimate a critical current density J_c from the experimentally observed field scale and the film thickness using $H_s=J_c d/\pi$.

A similar scaling was also observed in data taken from a ring resonator. Calculations of $\overline{|B(H)|}$ for the case a superconducting disk using the results of Ref. 15 cannot be distinguished from the $\ln\cosh(H/H_{s,\mathrm{strip}})$ behavior of the strip within experimental uncertainty, although the relation of the scaling field $H_{s,\mathrm{disk}}$ to J_c is different. We have presented the temperature dependence of $J_c(T)$ in Fig. 7 for the ring resonator, obtained using Eq. (10). (This overestimates the true J_c values by a factor of up to $\pi/2$, due to the ring geometry although the magnitudes are consistent.)

When combined with the J_c values estimated from the nonlinear response at high T on the same resonator from Ref. 3 it would appear that the two estimates are consistent, and can well be described overall by a $(1-t^2)^2$ dependence reminiscent of a mean field thermodynamic critical field, H_c. Also the magnitudes obtained, $J_c(77\ \mathrm{K})\approx 2\times 10^6$ A/cm^2, comparable with independent dc measurements on films of the same batch.

To summarize, flux penetration into the virgin state for moderate fields is very well characterized quantitatively by the critical-state model for perpendicular geometry.

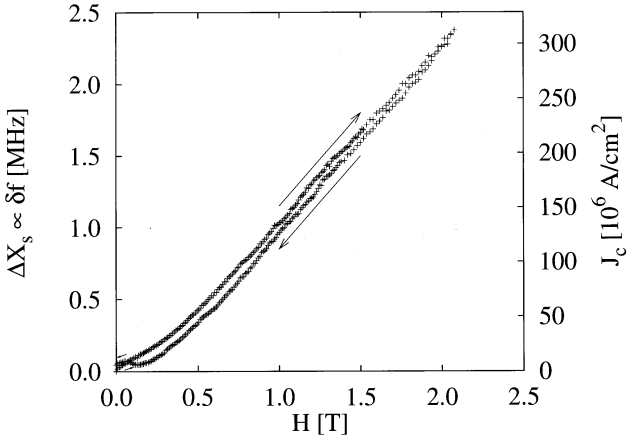

FIG. 8. Hysteretic response of $R_s(H)$ for $H_{\max}\gg H_s$. Results are presented for resonator N4 at 3.7 GHz and 10 K.

C. High-field response for $H\gg H_s$

For very high fields, much greater than the self-field H_s, the impedance becomes linear in the applied field. In this regime the slopes can be used to extract vortex parameters such as the pinning force constants and the viscosity as we have done in Ref. 2.

V. HYSTERESIS

So far we have only examined what happens as the externally applied magnetic field is slowly increased from zero. The response as the field is slowly reduced and also reversed will be discussed in this section.

A. Moderate-field hysteresis

The typical response when the applied field is ramped up to a field significantly higher than H_s and then reduced is presented in Fig. 8. As can immediately be seen this response is qualitatively different from that predicted by the critical-state model alone (presented in Fig. 3). The loop has the opposite handedness, and is much smaller than H_s in width. While the reduced width of the loop may be consistent with the presence of a geometrical or other barrier at the strip edge, the handedness however cannot be so easily explained.

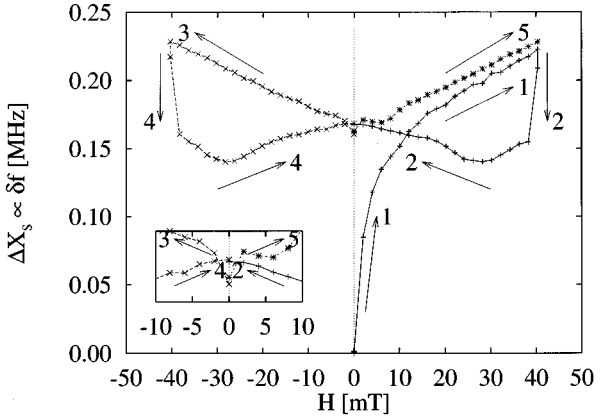

FIG. 9. Hysteretic response of $X_s(H)$ for $H_{\max}\sim H_i$. Results are presented for resonator N4 at 3.7 GHz and 35 K.

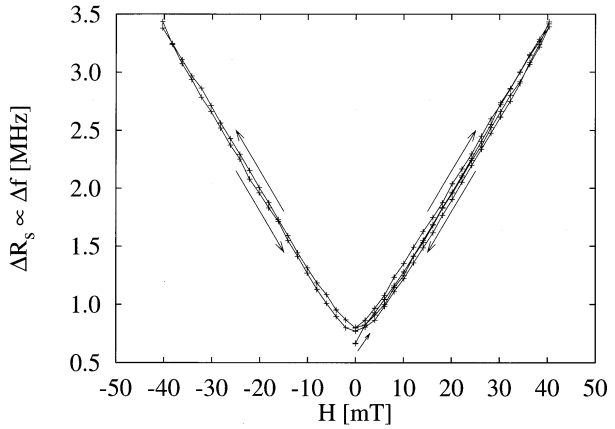

FIG. 10. Low-field hysteresis in $R_s(H)$ at high temperatures. Results are presented for resonator N4 at 3.7 GHz and 84 K.

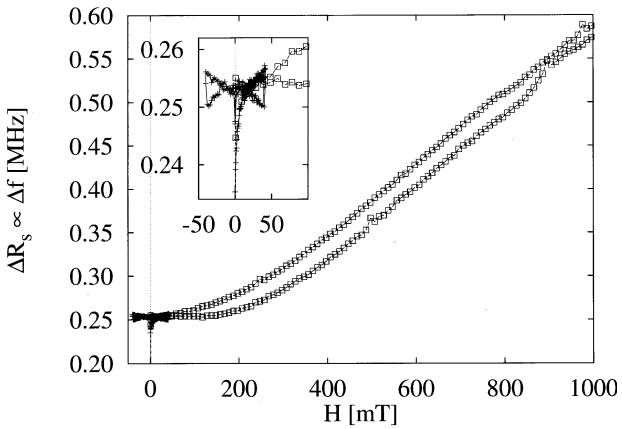

FIG. 11. Magnified view of the hysteresis data for R_s presented in Fig. 8 for moderate fields and low fields (inset).

There are a number of possible ways to explain this behavior: The relationship between $\tilde{Z}_s$ and $\overline{|B(H)|}$ does not apply, the construction [Eq. (5)] used to determine $B_{\downarrow}(H)$ does not apply, or a fraction of the flux, principally at the edges, is sufficiently weakly pinned to be able to leave the sample quickly as the applied field is reduced.

B. Hysteresis at very low field

In order to shed some light on the issue, we have also carried out measurements of the hysteretic response for fields $\sim H_i$. Typical response when the applied field is ramped up to a field $H_{\max}$ comparable to H_i and then down to $-H_{\max}$ and finally increased back to $H_{\max}$ is presented in Fig. 9. Although only $\Delta X_s(H)$ is presented in the figure, $\Delta R_s(H)$ has qualitatively the same behavior. At sufficiently high T, response qualitatively similar to that observed in the previous section is recovered even for fields $|H|<40$ mT (see Fig. 10).

To put these effects into perspective, Fig. 11 presents the data of Fig. 8, along with low-field data obtained at the same temperature. Note that the magnitude of these effects is very small, and requires extreme care to be observed.

Clearly the clockwise nature of the hysteresis initially observed at high fields is preserved even at these low-field scales, and the drop in $\tilde{Z}_s$ as the applied field is reduced appears to be rather sudden, taking place within <1 mT.

Below we summarize the essential features of the hysteretic response.

Sudden drop in both R_s and X_s as the applied field is reduced, below even the virgin state response.

After $H_{\max}$ is reached, the response is clearly symmetric in H about $H=0$.

$\tilde{Z}_s$ at $H=0$ does not return to its initial value in the normal state.

A cusplike feature is observed as H is increased in the opposite direction after reaching $H=0$ (Fig. 11).

A cusplike feature is expected in magnetization as the field crosses $H=0$ in the presence of a geometrical barrier.[14] One must also keep in mind that the time taken to manually switch the current leads (to reverse the field) was finite in these experiments so that any time dependence (such as flux creep) may also be a possible source for the observed cusp.

C. Comparison to dc magnetization

Hysteresis loops from dc magnetization measurements on thin films and bulk polycrystalline samples in high fields ($H>\sim 1$ T) generally appear quite different from those we report here, and are often more consistent with critical state models. $M(H)$ loops are generally counterclockwise and estimates of $J_c(H)$ are routinely extracted from the directly from the loop width. Measurements on single crystalline samples also have the ''correct'' handedness although the fishtail effect is observed in the vast majority of samples.

This is in contrast to the results presented here where the hysteresis loops have the opposite handedness are much narrower than expected from the critical-state model. In fact, rather than being related to H_s, the hysteresis width appears to be governed by a field scale on the order of H_i.

VI. CONCLUSION

The linear electrodynamic response of vortices in thin films in the perpendicular geometry has been investigated within the framework of recent theoretical work. While flux entry into a sample initially in the virgin state appears to be well described by the critical-state model, flux exit when the field is reversed does not follow the model. The expected hysteresis from the critical-state model (of magnitude $\approx 2H_s$), is *not* observed. In fact, the observed behavior would imply that the absolute flux density $\overline{|B(H)|}$ drops suddenly as the applied magnetic field is reduced. The applicability of two-level critical-state models[28] often used to explain similar hysteresis curves in bulk ceramic material[29] will be examined in the future.[30] The presence of geometrical barriers at the strip edges can help to reduce the level of hysteresis expected,[17] but will not lead to the observed response. Other models which predict a nonlinear dependence of the microwave response on dc magnetic fields will also be considered.[31]

ACKNOWLEDGMENTS

This work was supported by Rome Laboratory and the NSF through Grants No. NSF-DMR-9223850 and No. NSF-DMR-9623720. The authors thank R. S. Markiewicz and D. P. Choudhury for useful discussions and José Silva for his technical assistance.

*Present address: Superconductor Technologies, Inc., Santa Barbara, CA.
[1] A. Forkl, Phys. Scr. **T49**, 148 (1993).
[2] B. A. Willemsen, S. Sridhar, J. S. Derov, and J. H. Silva, Appl. Phys. Lett. **67**, 551 (1995).
[3] B. A. Willemsen, J. S. Derov, J. H. Silva, and S. Sridhar, IEEE Trans. Appl. Supercond. **5**, 1753 (1995).
[4] J. I. Gittleman and B. Rosenblum, Phys. Rev. Lett. **16**, 734 (1966).
[5] M. W. Coffey and J. R. Clem, Phys. Rev. Lett. **67**, 386 (1991).
[6] J. Owliaei, S. Sridhar, and J. Talvacchio, Phys. Rev. Lett. **69**, 3366 (1992).
[7] D.-H. Wu, and S. Sridhar, Phys. Rev. Lett. **65**, 2074 (1990).
[8] S. Sridhar, B. Maheswaran, B. A. Willemsen, D. H. Wu, and R. C. Haddon, Phys. Rev. Lett. **68**, 2220 (1992).
[9] S. Oxx, D. P. Choudhury, B. A. Willemsen, H. Srikanth, S. Sridhar, P. C. Canfield, and B. K. Cho, Physica C **264**, 103 (1996).
[10] C. P. Bean, Phys. Rev. Lett. **8**, 250 (1962).
[11] M. Tinkham, *Introduction to Superconductivity* (McGraw-Hill, New York, 1975).
[12] E. H. Brandt and M. Indenbom, Phys. Rev. B **48**, 12 893 (1993).
[13] M. Darwin, J. Deak, L. Hou, M. McElfresh, E. Zeldov, J. R. Clem, and M. Indenbom, Phys. Rev. B **48**, 13 192 (1993).
[14] E. Zeldov, A. I. Larkin, V. B. Geshkenbein, M. Konczykowski, D. Majer, B. Khaykovich, V. M. Vinokur, and H. Shtrikman, Phys. Rev. Lett. **73**, 1428 (1994).
[15] J. R. Clem and A. Sanchez, Phys. Rev. B **50**, 9355 (1994).
[16] W. T. Norris, J. Phys. D **3**, 489 (1970).
[17] E. Zeldov, A. I. Larkin, M. Konczykowski, B. Khaykovich, D. Majer, V. B. Geshkenbein, and V. M. Vinokur, Physica C **235-240**, 2761 (1994).
[18] A. B. Pippard, Proc. R. Soc. London, Ser. A **203**, 210 (1950).
[19] B. D. Josephson, J. Phys. F **4**, 751 (1974).
[20] D.-H. Wu, C. A. Shiffman, and S. Sridhar, Phys. Rev. B **38**, R9311 (1988).
[21] S. K. Yip and J. A. Sauls, Phys. Rev. Lett. **69**, 2264 (1992).
[22] R. Liang, P. Dosanjh, D. A. Bonn, W. N. Hardy, and A. Berlinsky, Phys. Rev. B **50**, 4212 (1994).
[23] T. L. Hylton, A. Kapitulnik, M. R. Beasley, J. P. Carini, L. Drabeck, and G. Grüner, Appl. Phys. Lett. **53**, 1343 (1988).
[24] P. P. Nguyen, D. E. Oates, G. Dresselhaus, and M. S. Dresselhaus, Phys. Rev. B **48**, 6400 (1993).
[25] J. Halbritter, J. Appl. Phys. **71**, 339 (1992).
[26] A. M. Portis, D. W. Cooke, E. R. Gray, P. N. Arendt, C. L. Bohn, J. R. Delayen, C. T. Roche, M. Hein, N. Klein, G. Müller, S. Orbach, and H. Piel, Appl. Phys. Lett. **58**, 307 (1991).
[27] M. Golosovsky, M. Tsindlekht, and D. Davidov, Supercond. Sci. Technol. **9**, 1 (1996).
[28] L. Ji, M. S. Rzchowski, N. Anand, and M. Tinkham, Phys. Rev. B **47**, 470 (1993).
[29] V. S. Bai, P. Patanjali, S. M. Bhagat, and S. Tyagi, J. Supercond. **8**, 299 (1995).
[30] D. P. Choudhury *et al.* (unpublished).
[31] B. Placais, P. Mathieu, Y. Simon, E. B. Sonin, and K. B. Traito, Phys. Rev. B **54**, 13 083 (1996).